J Mater Sci (2006) 41:5548–5555
DOI 10.1007/s10853-006-0335-x

Investigations on the high cycle fatigue behaviour of stir cast AA 6061-SiC_p composites

K. Mahadevan · K. Raghukandan · T. Senthilvelan · B. C. Pai · U. T. S. Pillai

Received: 17 June 2004 / Accepted: 15 September 2005 / Published online: 20 June 2006

Abstract The room temperature high cycle fatigue behaviour of stir cast AA 6061-SiC_p composites, with varying reinforcement percentage, is studied. The specimens were tested under fully reversed cyclic deformation in the peak aged condition. Composite with 20% reinforcement exhibit superior fatigue strength over other composites (with 10,15 and 25% reinforcement). The experimental results are correlated with scanning electron micrographs of the failed specimens. Two distinct morphologies namely, crack initiation/ propagation and fast fracture region, were present. Mode-I type cracking was found to have dominated the crack initiation. The final fracture mode was found to be ductile with nucleation, growth and coalescence of cracks in the matrix.

Introduction

The development of metal matrix composites (MMCs) has been one of the major innovations in the field of materials in the past 20 years. The early MMCs were made with continuous fiber reinforcement, and while work in this area continues, it was soon apparent that the cost of continuous fibers, complex fabrication routes, and limited fabricability, would restrict their use to those applications requiring the ultimate performance [1]. This led to the development of discontinuously reinforced composites (DRCs), particularly of aluminium matrix reinforced with Al_2O_3 and SiC particles. This class of DRCs, though offering only modest changes in properties, are more isotropic in nature and have good potential to be used as low cost substitutional material for a wide spectrum of applications [2]. In particular, the reduction in operating cost due to weight saving in ground transportation is considerably less when compared to avionics or aerospace industries. This relatively lower premium on weight saving compels the automobile industries to look for mass production of cheaper alternative materials, with reproducible properties. In this context, the liquid state processed DRCs seem to be a prospective substitution material for the automotive sector [3]. Among the DRCs the most common particulate composite system is the aluminium matrix reinforced with SiC particles [4]. Moreover, out of the various liquid state routes for processing of these DRCs, stir-casting technique appears to be a promising method for the mass production with reproducible properties at a less cost [4].

Apart from the encouraging static properties, one important design criterion in the usage of DRCs is their fatigue resistance, particularly so in automotive industry, where High Cycle Fatigue (HCF) resistance is often demanded [5]. A limited number of experimental studies have been conducted to determine the HCF behaviour of solid and liquid state processed DRCs [6–10]. These studies concluded that, in general, as in other metallic materials, fatigue life of DRCs under HCF conditions involves crack nucleation and propagation. Many investigators [11–14] have reported that when stress-controlled (HCF) experiments are used to characterize fatigue, the

K. Mahadevan (✉) · T. Senthilvelan
Department of Mechanical Engineering, Pondicherry Engineering College, Pondicherry 605 014, India
e-mail: kayyem@yahoo.com

K. Raghukandan
Department of Manufacturing Engineering, Annamalai University, Annamalai Nagar 608 002, India

B. C. Pai · U. T. S. Pillai
Metals Processing Division, Regional Research Laboratory, Thiruvananthapuram 695 019, India

fatigue lives of DRCs are superior to those of un-reinforced metals. These improvements are significantly pronounced at lower stresses, in the high cycle fatigue regime, while at high stresses, the differences in the properties of the DRCs and un-reinforced materials are reduced.

Bonnen et al. [13] reported that cracks in the aluminium matrix DRCs with high volume fraction of reinforcement initiated near the particle/matrix interface, or by the fracture of individual particles, stressed more than particles completely embedded within the matrix. Moreover, fatigue crack initiation and failure in these DRCs are more likely to take place at defects at the surface of the specimen. Chen et al. [15] reported that in the low stress range, crack originated early in fatigue life, at approximately 10% of total life [15]. On the contrary, in high stress range, the crack initiation occurred at a later stage. Therefore, in the low stress range crack propagation was dominant, while at high stress range crack initiation was more important in determining fatigue life.

Fatigue crack propagation rates for SiC particulate reinforced aluminium composites containing fine SiC particles were higher than those for the un-reinforced matrix alloys in a given stress intensity factor range, Δk. The fatigue crack propagation properties for those DRCs containing coarse SiC particles were very similar to that of the matrix alloy [6]. Moreover, experimental studies demonstrated that the overall HCF performance as well as the fatigue limit of DRCs improved with the reinforcement volume fraction [8, 16, 17]. These changes were generally associated with an increase in the number of cycles to initiate a crack and in some cases [18, 19] it was reported that the fatigue strength of DRCs decreased with the addition of reinforcement. The above discrepancy is attributed to the many microstructural variables influencing [7] the fatigue properties of the DRCs. Therefore, an in depth understanding on the effects of these variables is required for the extensive applications of DRCs. Further, most of the earlier works [6–14] have been done based on the availability of the DRCs rather than the variables itself. Thus it has been difficult to clarify the general role of microstructural factors in fatigue strength of DRCs. Hence in the present study an attempt has been made to investigate the effect of reinforcing particles on the HCF behaviour of stir cast AA 6061-SiC_p composites and the results are compared with that of the un-reinforced alloy processed by the same technique.

Experimental procedure

AA 6061-SiC_p DRCs reinforced with 10,15,20 and 25% (by weight) of SiC particles were examined in this study. The reinforcing SiC particles of average size of 23 microns were introduced into the vortex created by mechanical stirring of the metal matrix through a separate chute. Details of the stir casting process for fabricating DRCs is described elsewhere [4]. The chemical composition of the AA 6061 aluminium alloy used in the present study is given in Table 1. The cast billets, 75 mm in diameter were hot extruded at 420 °C to rods of 17 mm diameter in four stages using conical type extrusion dies. Figures 1 and 2 shows the microstructures of the extruded DRCs with 20% and 25% reinforcement.

Table 1 Nominal composition (wt%) of matrix alloy AA 6061 tested

Si	Fe	Cu	Mn	Mg	Zn	A1
0.4–0.8	<0.7	0.15–0.41	0.15	0.82–1.2	0.25	Balance

From the microstructure Fig. 1(a, b) it is observed that for DRC with 20% reinforcement the SiC particles are distributed uniformly in the aluminium matrix. The absence of blow holes, macropores and gravity settling of SiC in aluminium matrix indicate the suitability of the casting process adopted. Moreover, some preferential alignment of the reinforcement particles along the extrusion axis is also seen in Figs. 1(b) and 2(b). In the DRC with 25% reinforcement (Fig. 2(a, b)), agglomerated sites, consisting of a few large sized SiC particulates, intermingled with smaller, uniform and more regularly shaped particles, were observed resulting in particle rich and

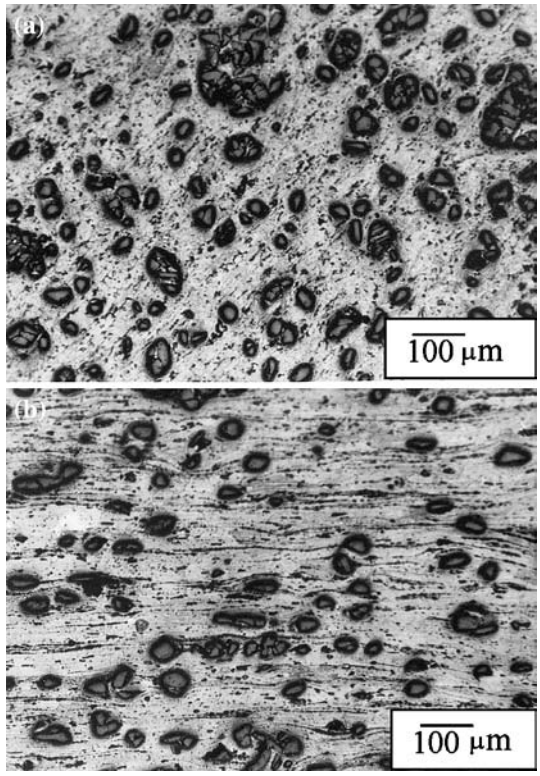

Fig. 1 Micrographs of the extruded AA 6061-SiC_p composite with 20% reinforcement (**a**) transverse (**b**) longitudinal

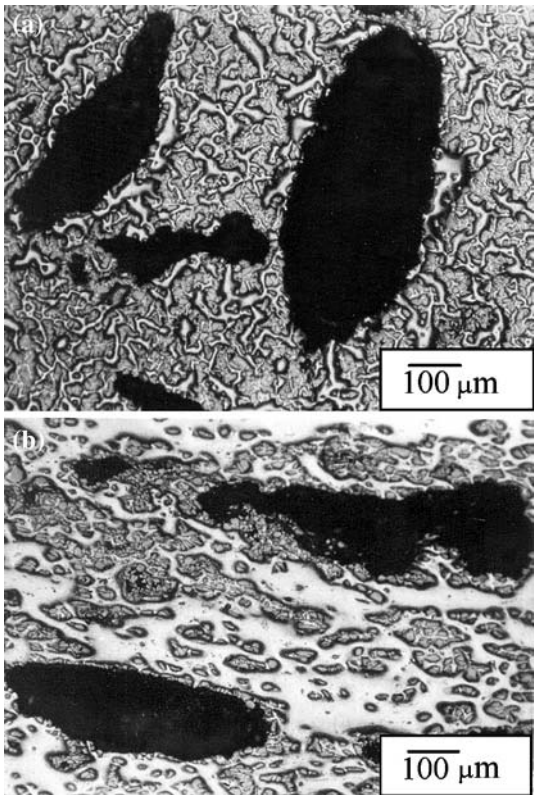

Fig. 2 Micrographs of the extruded AA 6061-SiC_p composite with 25% reinforcement (**a**) transverse(**b**) longitudinal

particle depleted regions. Apart from this, few intermetallic inclusions that were formed as a result of the casting process is also seen. These inclusions are visible as small dark particles, which were not dissolved in the matrix. Table 2 compiles the static properties of the extruded DRCs and the un-reinforced alloy before heat treatment.

Smooth specimens of appropriate dimensions as per ISO: 1143–1975 was prepared from the extruded bars of DRCs for rotating bending fatigue testing. Toroidal specimens of gauge section of length 50 mm and 8 mm diameter at the centre were heat treated by solutionizing for 3 h at 530 °C followed by water quenching and artificial aging for 4 h at 170 °C [20]. Specimens of similar shape and dimensions were also prepared from the extruded un-reinforced alloy. These specimens were subjected to heat treatment as per T6 condition and were tested for comparison purpose. The properties of the DRCs and un-reinforced alloy after heat treatment were tabulated in

Table 3 Properties of heat treated AA 6061-SiC_p composites/un-reinforced alloy

Specification	Ultimate tensile strength [Mpa]	% Elongation	Hardness [BHN]
AA6061	311	12	75
AA6061/SiC/10p	310	6.0	98
AA6061/SiC/15p	346	5.0	103
AA6061/SiC/20p	478	4.0	107
AA6061/SiC/25p	467	2.0	120

Table 3. The test specimen surface preparation followed a set of procedure. In the final stages of machining a feed rate of 0.01 mm/rev was used to remove 0.1 mm of material in the gauge length. Each specimen was then polished longitudinally, using successive grade of abrasive paper to remove a final 0.04 mm of material and to impart a surface finish of 0.025 μm C.L.A. The fatigue tests were carried out in the ETS INTRALAKEN rotating bending fatigue testing machine in laboratory environment at 2900 rpm. Three specimens were tested for each stress level selected and the average was taken for plotting of S–N curves. The fatigue fracture surfaces were examined using a scanning electron microscope.

Results

Figure 3 shows the plot of stress amplitude vs. cycles to failure for the DRCs with varying reinforcement volume fractions. Increasing the SiC particle fraction resulted in higher fatigue strength (taken as the highest stress at which a specimen survived 10^7 cycles) up to 20% reinforcement. However, the fatigue strength of the DRC with 25% reinforcement was slightly lesser than that of DRC with 20% reinforcement. This is in slight deviation from the earlier works [21, 22], which has reported an increase in fatigue strength with higher reinforcement fraction. In the present study this deviation in terms of reduction in the fatigue strength of DRC with 25% reinforcement may be attributed to early crack nucleation. In particular, DRC with 20% reinforcement showed a pronounced improvement in fatigue strength.

The stress vs. cycles to failure curves also showed an apparent convergence in fatigue lives of the DRCs at high stresses, which may be attributed to the lower ductility in

Table 2 Specification and static properties of extruded AA 6061-SiC_p composites/un-reinforced alloy

Specification	Nominal percentage of reinforcement (Wt. %)	Average particle size (μm)	Ultimate tensile strength (MPa)	% Elongation	Hardness (BHN)
AA6061	–	–	290	16	60
AA6061/SiC/10p	10	23	286	7	60
AA6061/SiC/15p	15	23	298	6	62
AA6061/SiC/20p	20	23	321	5	66
AA6061/SiC/25p	25	23	314	3	70

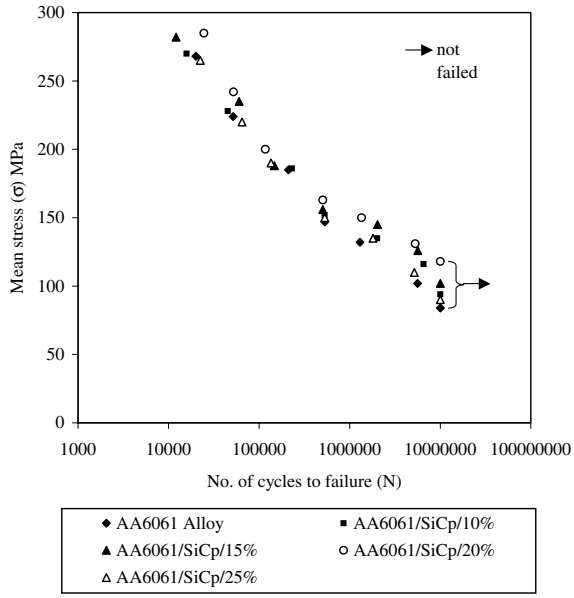

Fig. 3 Effect of SiC_p % reinforcement fraction on fatigue life

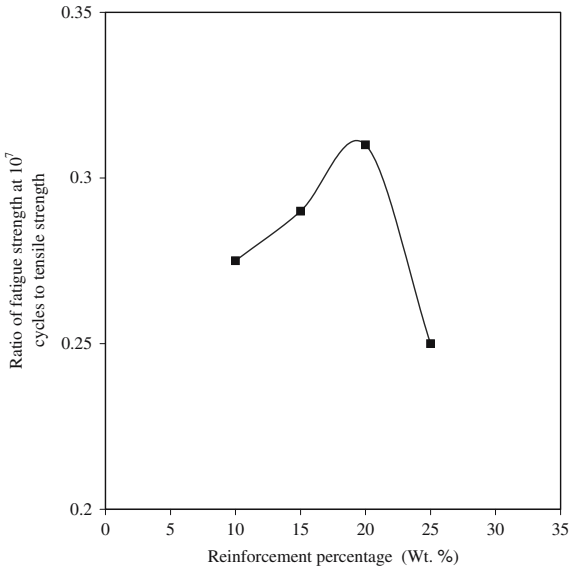

Fig. 5 Relationship between the ratios of the fatigue strength to tensile strength and the reinforcement fractions for T_6 conditions

the DRCs, i.e. ductility exhaustion. At high plastic strains (i.e. short lives) the cyclic ductility of a material limits the amount of plastic strain and thus, the number of cycles that can be accumulated prior to fracture. Therefore, at high stresses, as the plastic strains are lower in the DRCs, so too are the cyclic ductility and the resistance to cyclic strains. Moreover, a wide scatter in the results especially at low stress level is also noted as compared to higher stress levels, as in metallic materials.

Figure 4 shows the variation between the ratios of fatigue strength of DRCs σ_c, to the un-reinforced alloy σ_A, σ_C/σ_A at the number of cycles to failure at 10^7 cycles and the

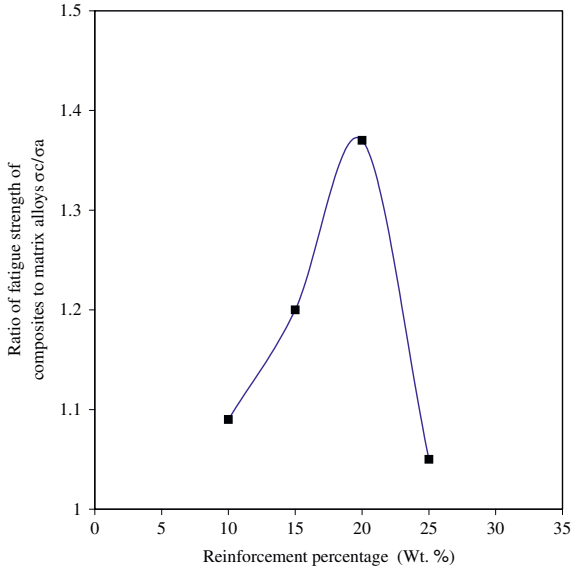

Fig. 4 Variation of ratio of fatigue strengths of DRCs to matrix alloy to the SiC_p reinforcement fraction

percentage of SiC_p reinforcement. The fatigue ratio tends to increase with an increase in the fraction of SiC reinforcement and reaches a peak for 20%. However, for DRC with of 25% reinforcement the value is slightly higher than that of the matrix alloy, which is ascribed to the early nucleation of cracks in the matrix.

Similarly Fig. 5 shows the variation of the ratio of fatigue strengths at 10^7 cycles (σ_C/σ_A), to the tensile strength (σ_T), and the percentage of SiC_p reinforcement. The data obtained in this study were distributed in the range of 0.25–0.3 while the earlier work on DRCs (processed through P/M route) has reported a value of about 0.38 [23]. In the present work, the lowest value was for the DRC with 25% reinforcement than other DRCs due to the early fatigue crack initiation at particle clustering beneath the specimen surface. Figure 6 shows the plot of endurance limit (taken at 10^7 cycles) and percentage of SiC_p reinforcement. The endurance limit increases with an increase in the percentage of reinforcement up to 20%. For the DRCs, with 25% reinforcement, the presence of SiC particle clusters in the matrix causes reduction in the endurance limit.

From the SEM fractograph Fig. 7, of the failed specimen with 20% reinforcement two distinct fracture morphologies were observed: a propagation region and a fast fracture region. In the propagation region equispaced striation marks oriented perpendicular to the direction of crack propagation are visible. The fast fracture region is relatively rough with the presence of ductile dimples. For DRC with 25% reinforcement Fig. 8 more than one crack propagation region was observed. This observation indicates that the above DRC contained more number of

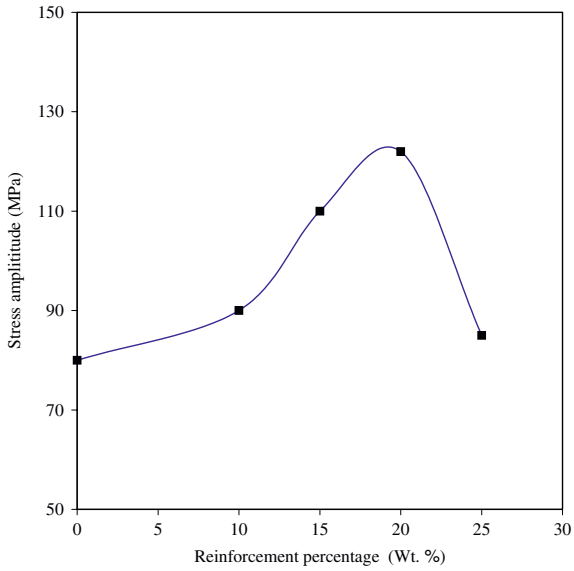

Fig. 6 Endurance limit (at 10^7 cycles) vs. % of SiC_p reinforcement

stress concentration regions, which has favoured an early nucleation of crack when compared to other DRCs.

Moreover, in the DRC with 25% reinforcement the inclusions (Fig. 9) assumed to have originated during processing as well as the particle clusters (Fig. 10) at the sub-surface have acted as early crack nucleation sites for fatigue fracture as reported by several other investigators [11, 21, 22]. Inclusions present in the matrix act as stress raisers and formation of particle clusters due to increase in % reinforcement results in lack of wetting leading to development of preferential crack initiation sites. Thus, from the above observation it is felt that stir casting process is suitable for processing of Al-SiC_p DRCs up to 20% reinforcement beyond which control of uniform distribution of SiC particles in the matrix becomes difficult. Figure 11(a–c) shows the SEM fractographs of the fatigue-failed specimens for 10, 15 and 20% reinforced DRCs in which voids or shrinkage holes were not observed. For

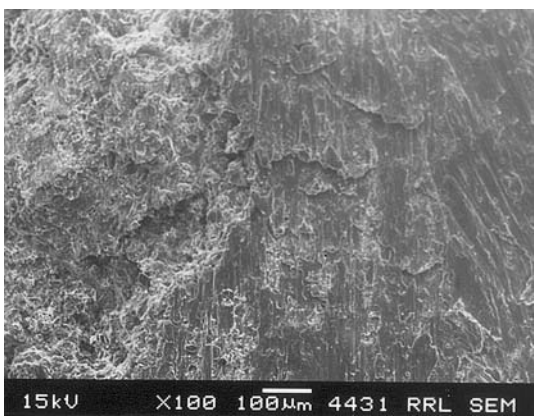

Fig. 7 SEM fractograph of AA 6061-SiC_p (20%) showing propagation and fast fracture regions

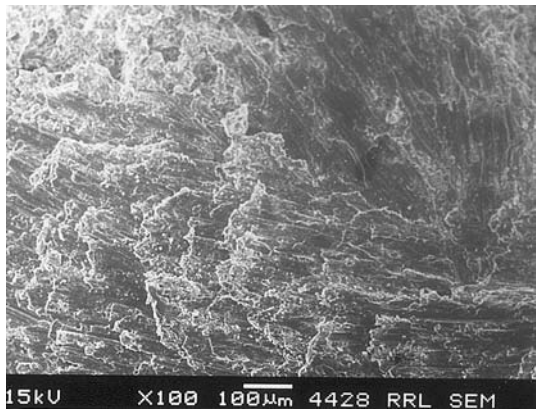

Fig. 8 SEM fractograph of AA 6061-SiC_p (25%) showing more than one crack propagation region

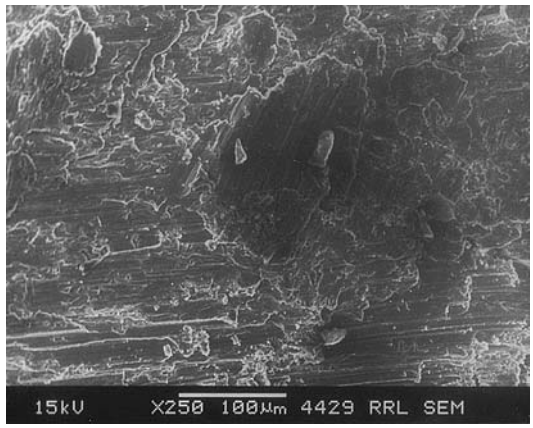

Fig. 9 SEM picture showing presence of inclusions in the (AA 6061-SiC_p/25%) matrix

these composites, Mode I type cracking (due to surface and sub-surface defects) was found to have dominated crack initiation. The fractured region exhibits a relatively smooth surface along with the presence of striation patterns. Since

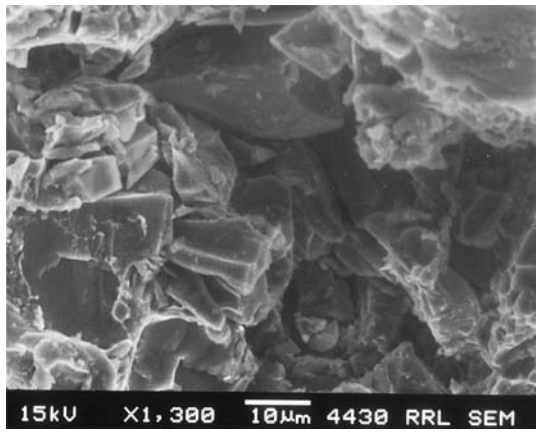

Fig. 10 SEM picture showing SiC particle clusters in the matrix of (AA 6061-SiC_p/25%)

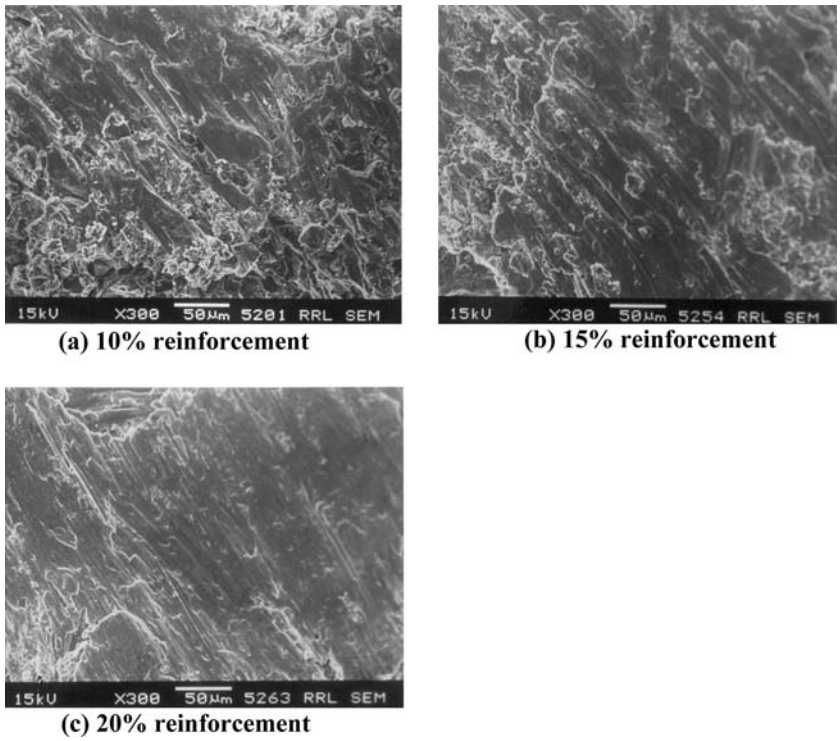

Fig. 11 SEM fractographs of fatigue failed AA 6061-SiC_p specimens (**a**) 10% reinforcement (**b**) 15% reinforcement (**c**) 20% reinforcement

the clarity of striation marks depends on the ductility of the matrix, from Fig. 11(a–c) it can be inferred that the type of fatigue fracture is more ductile in nature. Moreover, the appearance of dimples over the entire fractured region confirms the final fracture mode is also ductile.

Discussion

From the test results it is observed that, the fatigue strength of all DRCs (with 10, 15, 20 and 25% reinforcement) were superior to that of the un-reinforced alloy. However, among the DRCs, the composite with 20% reinforcement exhibit enhanced fatigue strength over others. In order, to fully understand fatigue mechanisms in DRCs, it is appropriate to discuss the increase in modulus and yield strength of the DRCs with respect to that of the un-reinforced alloy. The increase in modulus has been explained analytically and by the finite element method elsewhere [24, 25]. The explanation for the increase in yield strength in the DRCs, on the other hand, is not as simple. Arsenault and Wu [26] has attributed the increase in strength of the DRCs to the high dislocation density that arises from thermal mismatch between the DRCs constituents. Allison et al. [27] and Nardone and Prewo [28, 29] suggested that much of the strengthening comes from load transfer from the matrix to the reinforcement. Nardone and Prewo [28, 29] have used a modified shear-lag type of analysis, due to the small aspect ratio of the SiC particles, to show that load transfer from the matrix to the particles does exist. Using this analysis, the DRCs, yield strength, σ_c is given by [28]

$$\sigma_c = \sigma_m \left[\frac{V_p(S+4)}{4} + V_m \right] \quad (1)$$

where σ_m is the un-reinforced matrix yield strength, S is the aspect ratio of the reinforcement particle and V_p and V_m are the volume fractions of particles and matrix respectively.

A comparison of experimental and predicted yield strengths based on Eq. 1 is shown in Fig. 12. The predicted value is in good agreement with the experimental results. Thus, the modified shear-lag theory accurately predicts DRCs yield strength for this range of SiC volume fraction. Another contributing factor for the increase in fatigue strength may be related to the nature of slip in the matrix with increasing % reinforcement. If precipitates in the matrix are sheared by moving dislocations, strain localization reminiscent of persistent slip bands can occur since the precipitates are unable to resist any further deformation [30, 31]. It is likely that precipitate shearing occurs in the matrix due to small precipitate size and spacing [13, 32]. While the precipitates are deformable, the SiC particles are non-deformable, and act as obstacles to dislocation motion. A combination of non-deformable particles in a matrix of shearable precipitates can result in a beneficial change in the deformation mechanisms. According to Parker [30] this condition occurs when the microstructure consists of

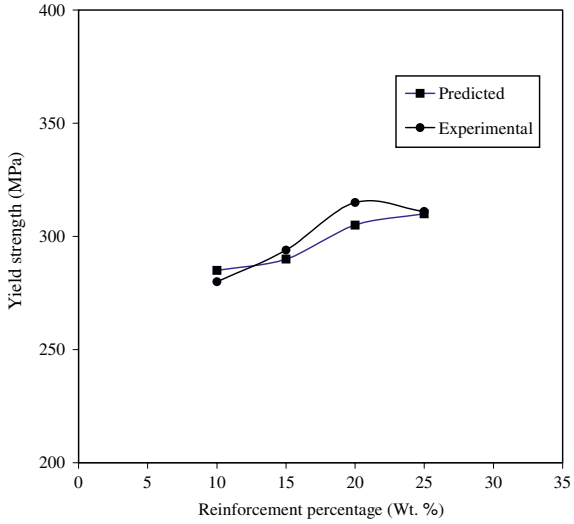

Fig. 12 Experimental and predicted yield strength

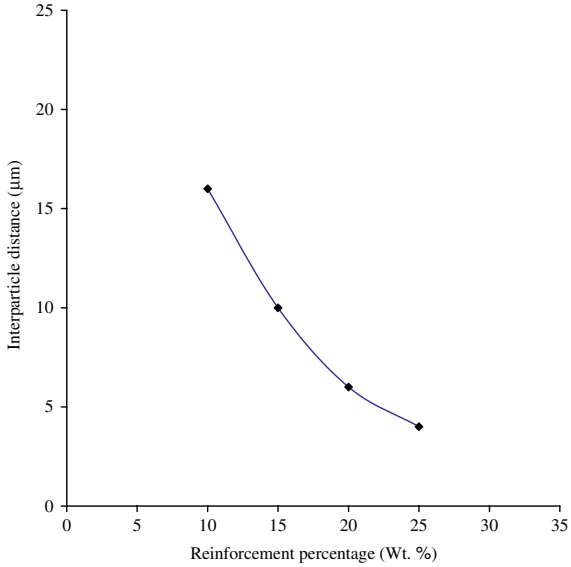

Fig. 13 Plot of theoretical values of reinforcement inter-particle spacing

non-deformable particles with a particle spacing of around 1 μm. The inter particle spacing, λ, between SiC particles in the present study (assuming uniform distribution of SiC particles in the matrix) is taken as the average centre to centre spacing between two particles less the particle diameter and is given by [33].

$$\lambda \approx d\left[\left(\frac{1}{2f}\right)^{1/3} - 1\right] \tag{2}$$

where d is the particle diameter and f is the volume fraction of particles. Figure 13 shows the calculated values for inter particle spacing in the matrix based on Eq. 2 for DRCs with 10, 15, 20 and 25% reinforcement. It is evident from Fig. 13 that, the inter particle spacing reduces and reaches the critical value of about 1 μm with increase in % reinforcement.

Thus with decreasing interparticle spacing up to the critical spacing, the fine precipitates give strength to the matrix while the larger SiC particles prevent the formation of reversible slip bands when the particles are spaced closely enough. Parker [30] also stated that the non deformable particles can act to stabilize the cell structure in the matrix at low strains, while with increasing strain, a sharpening of the cell wall structure takes place with slight disorientation across the cell walls. The fortuitous combination of closely spaced SiC particles, at large volume fractions and fine precipitates in the matrix of the DRCs may serve as an indirect strengthening mechanism.

For DRCs the interfacial bond strength between the matrix and the reinforcement plays a crucial role in the crack initiation process [6]. However, the interfacial bond strength depends on the morophology of the reinforcing particle and the processing route, which controls the degree of the reaction at the matrix. For the molten metal processed composites, the chances for formation of reaction products (Al_4C_3 and Silicon) is high, and subsequently the creation of a brittle zone in which interfacial failures are more likely to occur. The X-ray diffraction on the DRCs was performed using Cu $K\alpha$ radiation for phase identification. The peaks in the X-ray traces corresponds to the presence of aluminium and SiC. The absences of any significant reactive constituents are seen in the XRD Fig. 14.

Therefore, the chances of crack initiation at the SiC particle interface with the reaction products and the intermetalic particles forming a brittle zone aiding to interfacial failure are negligible. Hence, it can be stated that in DRCs with 10, 15 and 20% reinforcement, the surface crack initiation is impeded by the presence of uniformly distributed particles which are considered to act as barriers to the development of slip bands thus increasing the strength of the composites. Therefore, the initiation site shifts from the specimen surface to subsurface, when the concentrated stress exceeds the applied stress on the surface or else it originates at the surface defects similar to the un-reinforced alloy (Mode I crack by a slip deformation mechanism). On the other hand for DRC with 25% reinforcement, the main cause for the crack initiation is the presence of surface or subsurface particle clusters.

Conclusions

The fatigue strength of AA 6061-SiC_p particulate composites produced by stir casting was evaluated for four different % reinforcement. Results were compared with those of a AA 6061-T6 un-reinforced alloy produced by the same technique and the following conclusions were obtained.

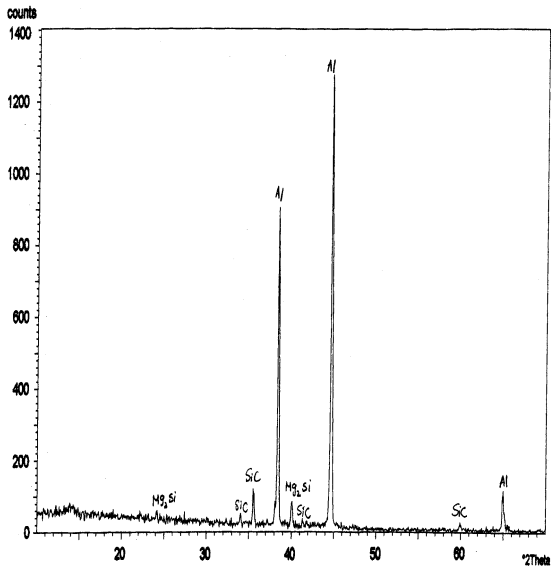

Fig. 14 XRD of the extruded AA 6061-SiC_p DRC

1. The fatigue strength of DRCs was superior when compared to that of the un-reinforced alloy. Among the DRCs the composite with 20% reinforcement had enhanced fatigue strength over others.
2. The ratio of the fatigue strength of DRCs to matrix alloy and % of SiC_p reinforcement were contained in the range of 1.10–1.37. The maximum value of 1.37 of fatigue ratio was obtained for DRC with 20% reinforcement.
3. The variation of the ratio of fatigue strength, to tensile strength $(\sigma_c/\sigma_A)/\sigma_T$ and % of SiC_p reinforcement were contained in the range of 0.25–0.31, higher than that of the un-reinforced alloy (0.25–0.28).
4. The endurance limit (taken at which a specimen survived 10^7 cycles) increases linearly with an increase in the % reinforcement from 10%–20%, but drops to a lower value for DRC with 25% reinforcement.
5. Two distinct morphologies were observed from the fatigue failed specimens: an initiation/ propagation region and a fast fracture region.
6. At low stress levels dimple patterns were observed on the whole fractured surface in the crack propagation region for all DRCs.
7. For specimens subjected to high stress levels the fractured region exhibits a relatively smooth surface along with the presence of striation patterns.
8. Except for DRC with 25% reinforcement, Mode-I type of cracking has found to be the cause for crack initiation.

Acknowledgements This research was supported by the Council of Scientific and Industrial Research, India (CSIR GRANT NO.70/(0043)/01/EMR-II). The authors are thankful to the Materials Processing Division, Regional Research Laboratory, Thiruvananthapuram, India for providing the materials used in this research work.

References

1. Mahadevan K, Raghukandan K, Venkatraman A, Pai BC, Pilai UTS (2003) Mat Sci Forum 437–438:223
2. Raghukandan K, Hokamoto K, Lee JS, Chiba A, Pai BC (2003) J Mat Sci Tech 19(4):341
3. Hashin J, Looney L, Hahmi MSJ (1999) J Mat Proc Tech 92–93:01
4. Pai BC, Pillai RM, Sathyanaranan KG, Sukumaran K, Pillai UTS, Pillai SGK, Ravikumar KU (2001) Met Mat Proc 13(2–4):225
5. Subrata R (1995) Bull Mater Sci 18(b):693
6. Chitoshi M, Tanaka Y, (1992) J Mat Sci 27:413
7. Shinji K, King JE, Knott JF (1991) Mat Sci Engg A146:317
8. Hurd NJ (1998) Mat Sci Tech 4:513
9. Poza P, Lorca L (1999) Met Mater Tran A 30A:857
10. Chawla N, Habel U, Shen YL, Andres C, John JW, Allison JE (2000) Met Mater Tran A 31A:531
11. Hall J, Johns TW, Sachdew (1994) Mater Sci Engg A A183:69
12. Han NL, Wang IG, Sun L (1995) Scripta Metall Mater 33:781
13. Bonnen JJ, Allison JE, Jones JW (1991) Met Mater Tran A 22A:1007
14. Vaidya AR, Lewandowski JJ (1996) Mater Sci Engg A A220:85
15. Chen EY, Lawson L, Meshii N (1995) Mater Sci Engg A A200:192
16. Chawla N, Andres C, Jones JW, Allison JE (1998) Metall Matrix Trans A 29A:2843
17. Lorca L, Blayce A, Yue TM (1991) Mater Sci Engg A134:247
18. Shang JK, Pitchie RO (1989) In: Arsenault RJ, Everette RK (eds) Metal matrix composites. Academic Press, Boston, MA, USA, p 255
19. Vyketek GM, Vanaken DC, Allison JE (1995) Met Mater Trans A 26A:3155
20. Mahadevan K, Rahukandan K, Senthilvelan T, Pai BC, Pillai UTS (2005) Mater Sci Engg A 396:188
21. Chang R, Morries WL, Buck O (1979) Scripta Mater 13:191
22. Williams DR, Fine ME (1985) In: Harrigan WC, Strige J, Dhingra AK (eds) Proceedings of the IV International Conference on Composite Materials. TMS, PA, USA, p 639
23. Harris SJ (1988) Mater Sci Tech 4:231
24. Lloyd DJ (1994) Int Mater Rev 39:1
25. Davis LC (1991) Met Mater Trans A 22A:3065
26. Arsenault RJ, Wu SB (1988) Scripta Metall 22:767
27. Allison IE, Davis LC, Jones JW (1997) In: Composites engineering handbook. Marcel Decker, NY, p 441
28. Nardone VC, Prewo KM (1986) Scripta Metall 20:43
29. Nardone VC, Prewo KM (1989) Scripta Metall 23:291
30. Parker BA (1989) In: Treatise on materials science and technology. Academic Press, Boston, USA, p 539
31. Johannesson B, Ogin SL, Sakiropoulos T (1991) In: Metal matrix composites-processing, microstructure and properties. Riso National Laboratory, Roskilde, Denmark, p 411
32. Allison JE, Jones JW (1993) In: Fundamentals of metal matrix composites. Butterworth-Heinemann, Stonehanns, MA, USA, p 269
33. Meyers, MA, Chawla KK (1999) In: Mechanical behaviour of materials. Prentice Hall, NJ, USA, p 493